Progress In Electromagnetics Research, Vol. 170, 63–78, 2021

Computational Investigation of Nanoscale Semiconductor Devices and Optoelectronic Devices from the Electromagnetics and Quantum Perspectives by the Finite Difference Time Domain Method

Huali Duan[1, 2], Wenxiao Fang[3], Wen-Yan Yin[1], Erping Li[1, 2], and Wenchao Chen[1, 2, *]

(*Invited Review*)

Abstract—In the simulation of high frequency nanoscale semiconductor devices in which electromagnetic (EM) fields and carrier transport are coupled, and optoelectronic devices in which strong interactions between EM fields and charged particles exist, both the Maxwell's equations and the time-dependent Schrödinger equation (TDSE) need to be solved to capture the interactions between EM and quantum mechanics (QM). One of the numerical simulation methods for solving these equations is the finite difference time domain (FDTD) method. In this review paper, the development of FDTD method applied in EM and QM simulation is discussed. Several widely used FDTD techniques, i.e., explicit, implicit, explicit staggered-time, and Chebyshev methods, for solving the TDSE are introduced and compared. The hybrid approaches based on FDTD method, which are used to solve the Poisson-TDSE and Maxwell-TDSE coupled equations for EM-QM simulation, are also discussed. Furthermore, the applications of these simulation methods for nanoscale semiconductor devices and optoelectronic devices are introduced. Finally, a conclusion is given.

1. INTRODUCTION

Comprehensive modeling and numerical simulation techniques for emerging nanoscale semiconductor devices and optoelectronic devices to capture the interactions between electromagnetics (EM) and quantum mechanics (QM) are necessary. For nanoscale semiconductor devices in which the operation frequency increases continuously, the quasi-static (QS) EM and time-dependent QM simulation are needed to obtain their high-frequency performance [1]. On the other hand, for optoelectronic devices such as quantum-dot (QD) lases and semiconductor optical amplifiers (SOAs) which have more complex interactions between EM fields and charged particles [2], the time-dependent EM-QM simulation is also needed to simulate their dynamic properties [3].

Maxwell's equations and time-dependent Schrödinger equation (TDSE) are the fundamental governing equations of EM and QM, respectively [4, 5]. In the time-dependent EM-QM simulation, the quantum transport can be simulated by solving the TDSE which incorporates the effect of EM fields through the magnetic vector potential "**A**" and the electrical scalar potential "Φ", as shown in Eq. (1). And the feedback from quantum transport to the EM fields can be modeled by adding quantum current density "J_q" obtained from the TDSE to Maxwell's equations, as shown in Eq. (2).

$$i\hbar\frac{\partial\Psi(r,t)}{\partial t} = \left[\frac{1}{2m}[-i\hbar\nabla - qA(r,t)]^2 + q\Phi(r,t) + V(r,t)\right]\Psi(r,t). \tag{1}$$

Received 22 December 2020, Accepted 20 January 2021, Scheduled 21 January 2021

* Corresponding author: Wenchao Chen (wenchaochen@zju.edu.cn).

[1] Innovative Institute of Electromagnetic Information and Electronic Integration (EIEI), College of Information Science and Electronic Engineering, Zhejiang University, Hangzhou 310027, China. [2] ZJU-UIUC Institute, International Campus, Zhejiang University, Haining 314400, China. [3] Science and Technology on Reliability Physics and Application of Electronic Component Laboratory, Guangzhou 510610, China.

$$\begin{cases} \nabla \times H = \dfrac{\partial D}{\partial t} + \sigma E + J_q. \\ \nabla \times E = -\dfrac{\partial B}{\partial t}. \end{cases} \tag{2}$$

Various numerical methods are developed for solving these equations, since the analytical solution is difficult to find especially for devices with complex structures [6–11]. For solving the TDSE, one of the numerical simulation methods is the finite difference time domain (FDTD) method which is also widely used in EM simulation [12]. In 2000, Sullivan applied FDTD method to solve one-dimensional (1D) TDSE [13], then developed this method to calculate two-electron wave packet dynamics in a QD modeled by a two-dimensional (2D) harmonic oscillator [14]. In 2002, Sullivan and Citrin presented a more flexible FDTD formulation of the TDSE, which is capable of simulating the dynamic processes in various nanostructures [15]. In 2004, the FDTD method applied for quantum applications was named as "FDTD-Q" by Soriano e al. With FDTD-Q method, the time behavior of the wave function for the quantum well wire (QWW) was obtained, and the analysis of stability and convergence of this method was also carried out [16]. Besides, there are also many modified methods proposed with better performance [17–21].

At low frequency, since QS approximation is valid, the Poisson's equation and time-independent Schrödinger equation are used to get the carrier transport properties of nanoscale semiconductor devices [22, 23]. However, as frequency increases, QS approximation is not accurate, and the time-dependent behavior should be taken into consideration. The Maxwell's equations and TDSE need to be solved to capture the interactions between EM and QM [3, 24, 25] and analyze the high frequency transient performances [26]. In 2007, Yang and Sui calculated the electron tunneling current through a potential barrier by 3D FDTD method to capture the EM-QM coupled behaviors [27]. In 2010, Ahmed et al. implemented a hybrid FDTD method to simulate the electric field distribution of the nanowire [28]. The hybrid approach, in which the conventional FDTD is used to solve the TDSE [12], and the locally one-dimensional FDTD (LOD-FDTD) is used to solve the Maxwell's equations [29, 30], is more efficient, and has more freedom to choose time step [31]. In 2018, a more efficient and precise FDTD method for the EM-QM simulation of single dipole, 2D quantum well (QW) and QD with current excitation was presented by Xiang et al., in which the fourth-order spatial differences are used for the whole device and third-order symplectic integrators are used for the TDSE [32]. And these numerical methods can be used for simulation of various nanoscale semiconductor devices and optoelectronic devices, such as plasmonic devices [33], QD lasers and amplifiers [3, 34, 35], and devices for quantum state control [36–38].

In this review paper, we present and discuss several different schemes of FDTD method for solving TDSE and hybrid approaches based on FDTD method for Poisson-TDSE and Maxwell-TDSE coupled equations, in which the corresponding stability condition and computational cost are discussed. Besides, simulation examples by FDTD methods, including nanoscale semiconductor devices and optoelectronic devices, are presented. Finally, a conclusion is given.

2. METHODOLOGY

2.1. FDTD for Time-Dependent QM Simulation

The TDSE can be solved by FDTD method to simulate time-dependent quantum transport. In this section, we introduce several different FDTD techniques for TDSE [39], i.e., explicit [40], implicit [41], explicit staggered-time [42] and one-step Chebyshev methods [43]. For simplicity, we start from the 1D case, and the discretization methods for 3D case can be obtained accordingly. The 1D TDSE is given by

$$i\hbar \frac{\partial \Psi(x,t)}{\partial t} = -\frac{\hbar^2}{2m} \frac{\partial^2 \Psi(x,t)}{\partial x^2} + V(x)\Psi(x,t). \tag{3}$$

2.1.1. Explicit Method

After using explicit second order difference scheme with central difference approximation [44], Eq. (3) can be discretized as

$$i\hbar\frac{\Psi_j^{n+1}-\Psi_j^{n-1}}{2\Delta t}=-\frac{\hbar^2}{2m}\frac{\Psi_{j-1}^n-2\Psi_j^n+\Psi_{j+1}^n}{\Delta x^2}+V_j\Psi_j^n, \tag{4}$$

where j represents the jth spatial grid, and the superscript n represents the nth temporal grid. Δx and Δt are the space step and time step, respectively. The explicit method is fast and easy to implement. When Δt satisfies Eq. (5), this explicit FDTD scheme is stable [45, 46].

$$\Delta t\leqslant\frac{\hbar}{\dfrac{2\hbar^2}{m\Delta x^2}+\max(|V|)}. \tag{5}$$

2.1.2. Implicit Method

The implicit difference scheme is also called Crank-Nicolson scheme and can be obtained by averaging the explicit forward difference scheme at time n and the backward difference scheme at time $n+1$ [41]. The discretized form of Eq. (3) can be written as

$$\Psi_{j+1}^{n+1}+(\alpha-2-\beta V_j)\,\Psi_j^{n+1}+\Psi_{j-1}^{n+1}=-\Psi_{j+1}^n+(\alpha+2+\beta V_j)\,\Psi_j^n-\Psi_{j-1}^n, \tag{6}$$

where $\alpha=i\frac{4m\Delta x^2}{\hbar\Delta t}$, $\beta=\frac{2m\Delta x^2}{\hbar^2}$. Such an implicit FDTD scheme is unconditionally stable and accurate [41]. From Eq. (6), we can see it is a tridiagonal set of linear equations. The computational cost of this scheme is very large, although there are many techniques for solving tridiagonal systems that can reduce the expense [47–49].

2.1.3. Explicit Staggered Method

The explicit staggered method has become a popular algorithm since it was first proposed by Visscher in 1991 [42]. In addition to retaining the advantages of explicit method, the explicit staggered method also improves the stability. Unlike the explicit and implicit method, the explicit staggered method treats the real and imaginary components of the wave function at staggered moments. The wave function can be described by

$$\Psi(x,t)=\Psi_R(x,t)+i\Psi_I(x,t), \tag{7}$$

where the subscripts R and I represent the real and imaginary components, respectively. Then, Eq. (3) can be rewritten as two partial differential equations as [42]

$$\hbar\frac{\partial\Psi_R}{\partial t}=-\frac{\hbar^2}{2m}\frac{\partial^2\Psi_I}{\partial x^2}+V\Psi_I, \tag{8}$$

$$\hbar\frac{\partial\Psi_I}{\partial t}=+\frac{\hbar^2}{2m}\frac{\partial^2\Psi_R}{\partial x^2}-V\Psi_R. \tag{9}$$

After defining the real and imaginary components at staggered moments, the above equations can be discretized as [42]

$$\Psi_{Rj}^{n+1}=\Psi_{Rj}^n-\frac{\hbar\Delta t}{2m\Delta x^2}\left(\Psi_{Ij-1}^{n+\frac{1}{2}}-2\Psi_{Ij}^{n+\frac{1}{2}}+\Psi_{Ij+1}^{n+\frac{1}{2}}\right)+\frac{\Delta t}{\hbar}V_j\Psi_{Ij}^{n+\frac{1}{2}}, \tag{10}$$

$$\Psi_{Ij}^{n+\frac{1}{2}}=\Psi_{Ij}^{n-\frac{1}{2}}+\frac{\hbar\Delta t}{2m\Delta x^2}\left(\Psi_{Rj-1}^n-2\Psi_{Rj}^n+\Psi_{Rj+1}^n\right)-\frac{\Delta t}{\hbar}V_j\Psi_{Rj}^n. \tag{11}$$

The two equations can be solved in an iterative way [42]. The explicit staggered method is stable when Δt satisfies the following equation [16]

$$\Delta t\leqslant\frac{\hbar}{\dfrac{\hbar^2}{m\Delta x^2}+\max(|V|)}. \tag{12}$$

Compared with Eq. (5), it is seen that when the potential is zero and all other variables are the same, the critical time step of this scheme is twice of that of the explicit method. Therefore, this method is more stable than explicit method when the time step is the same.

2.1.4. One-Step Chebyshev Method

The Chebyshev method is unconditionally stable [46], and large time step can be used in this method, but we need to carefully choose the time step due to the tradeoff between efficiency and accuracy. Rewrite the TDSE with Hamiltonian operator as

$$i\hbar\frac{\partial\Psi(x,t)}{\partial t} = H\Psi(x,t), \tag{13}$$

where $H = -\frac{\hbar^2}{2m}\frac{\partial^2}{\partial x^2} + V$. The general solution of Eq. (13) is given by

$$\Psi(t+\Delta t) = \exp\left(-\frac{i}{\hbar}H\Delta t\right)\Psi(t). \tag{14}$$

The key of this approach is to use a Chebyshev polynomial expansion to approximate the operator $\exp\left(-\frac{i}{\hbar}H\Delta t\right)$. By the way, Taylor expansion would lead to the explicit method [43]. After expanding the right-hand side of Eq. (14), we can obtain [43]

$$\Psi(t+\Delta t) = \mathrm{e}^{izB}\Psi(t) = \left[J_0(z) + 2\sum_{k=1}^{\infty} i^k J_k(z)T_k(B)\right]\Psi(t), \tag{15}$$

where $J_k(z)$ is the k order Bessel function, and $T_k(B)$ is a matrix-valued Chebyshev polynomial defined by the following relations [43]

$$T_0(B)\Psi(t) = \Psi(t), \quad T_1(B)\Psi(t) = B\Psi(t), \tag{16}$$

$$T_{k+1}(B)\Psi(t) = 2BT_k(B)\Psi(t) - T_{k-1}(B)\Psi(t), \quad k = 1, 2, \cdots \tag{17}$$

The way to improve the accuracy of this approach is mainly through increasing the expansion order, which is different from the previous approaches. The major drawback of this technique is that the potential distribution is supposed to be unvaried during each time step. When the potential is time-dependent, the time step will be limited by the speed of potential variation [39], thus, greatly reducing the efficiency of this technique. In addition, there are also many other approaches based on the above FDTD methods for further modifications [17–20].

2.2. FDTD for Time-Dependent EM-QM Simulation

Maxwell's equations and TDSE are the fundamental governing equations for EM and QM. A general model for time-dependent EM-QM simulation is shown in Fig. 1. The moving carriers inside the device

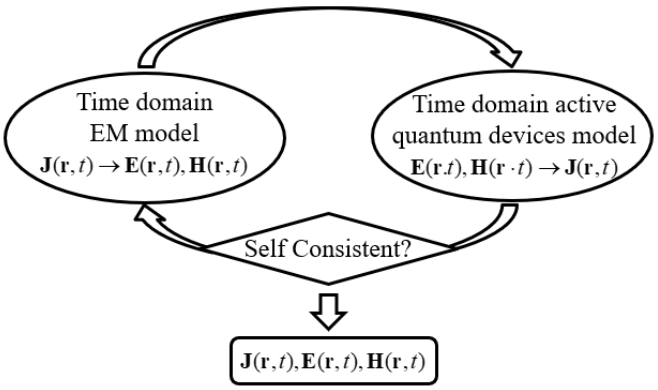

Figure 1. A general model for the coupled EM-QM simulation [50].

are the source of EM fields. The EM fields, in turn, will affect carrier transport. The impact of EM fields on the carriers is implemented by introducing the magnetic vector potential "**A**" and the electrical scalar potential "Φ" into the TDSE. And the current density "J_q" inside the device which is calculated by using the wave functions obtained from TDSE is incorporated into the Maxwell's equations to model the feedback from carriers to the EM fields. These terms establish the coupling between the time domain EM model and active quantum devices model [51, 52]. In this section, we mainly focus on the FDTD method for solving the coupled Maxwell's equations and TDSE. It's worth noting that when the frequency is much smaller than the velocity of the wave propagation divided by length of the channel (which is ~ 100 THz for the simulated device with a channel length of 20 nm), the EM simulation can be simplified into an electrostatic problem [53]. In this case, the TDSE is solved self-consistently with the Poisson's equation instead of Maxwell's equations [1]. Correspondingly, the two equations are coupled by the charge density term which is obtained from TDSE.

2.2.1. FDTD for Poisson-TDSE Coupled Equations

For electrostatic EM simulation, the time-dependent quantum transport equation is solved self-consistently with the Poisson's equation. In 2006, Chen et al. used FDTD method to solve the TDSE with the electrostatic potential obtained from Poisson's equation, and the simulation process is shown in Fig. 2 [50]. The Poisson's equation is given by

$$\nabla \cdot \varepsilon \nabla V = -\rho_v, \tag{18}$$

where ρ_v is the charge density calculated by the wave function from the TDSE. The Poisson's equation can be solved with numerical techniques, such as finite difference method (FD) and finite element method (FEM). Under the electrostatic assumption, the TDSE can be simplified as

$$i\hbar \frac{\partial \Psi(r,t)}{\partial t} = -\frac{1}{2m^*}\hbar^2 \nabla^2 \Psi(r,t) + U(r,t)\Psi(r,t). \tag{19}$$

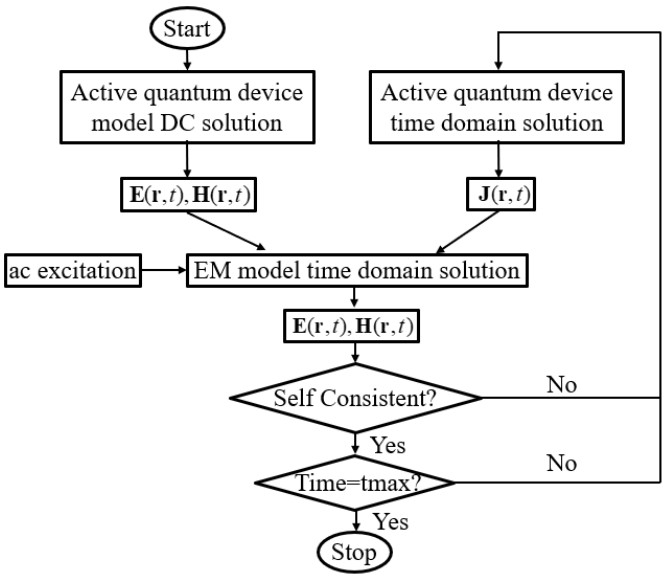

Figure 2. The process of electrostatic EM simulation with the time-dependent quantum transport [50].

The FDTD methods used to solve the TDSE have already described in the previous section. After getting the solution of this equation, we can obtain the charge density of the device which establishes the coupling between the TDSE and Poisson's equation as follows

$$\rho_v(z,t) = \frac{\sqrt{2m^*e}}{\pi\hbar} \int_{E_c}^{\infty} \frac{1}{\sqrt{E - E_c}} |\Psi(z,t)|^2 dE. \tag{20}$$

2.2.2. FDTD for Maxwell-TDSE Coupled Equations

For time-dependent EM-QM simulation at high frequency, the quantum transport properties are calculated by TDSE, and the EM field distribution is obtained from Maxwell's equations. In 2010, Ahmed et al. implemented a hybrid technique which consists of implicit and explicit FDTD methods for the simulation of nanowire with excitation source [28]. The side view and 3D structure of the nanowire are shown in Figs. 3(a) and (b). The conventional FDTD method is applied to the region with fine mesh where quantum effect exists, and LOD-FDTD is applied to the rest of the region with coarse mesh, as shown in Fig. 3(c) [28]. And the interpolation technique is used at the interface between the coarse and fine mesh domains to couple the two regions [54]. The Maxwell's equations containing the quantum current density are written as [55]

$$\nabla \times H = \frac{\partial D}{\partial t} + \sigma E + J_q, \tag{21}$$

$$\nabla \times E = -\frac{\partial B}{\partial t}, \tag{22}$$

where "J_q" can be obtained from the TDSE. The Maxwell's equations can be solved by LOD-FDTD method which consists of three sub time-steps defined by the general LOD procedure in the three spatial coordinate directions [30]. For simplicity, the first step equations of the LOD-FDTD method are given as follows, and the other two can be obtained similarly [30].

$$\frac{\partial B_x^{n+\frac{1}{3}}}{\partial t} = 0, \tag{23}$$

$$\frac{\partial B_y^{n+\frac{1}{3}}}{\partial t} = \left(\frac{\partial E_z^{n+\frac{1}{3}}}{\partial x} - \frac{\partial E_z^{n}}{\partial x} \right), \tag{24}$$

$$\frac{\partial B_z^{n+\frac{1}{3}}}{\partial t} = -\left(\frac{\partial E_y^{n+\frac{1}{3}}}{\partial x} - \frac{\partial E_y^{n}}{\partial x} \right), \tag{25}$$

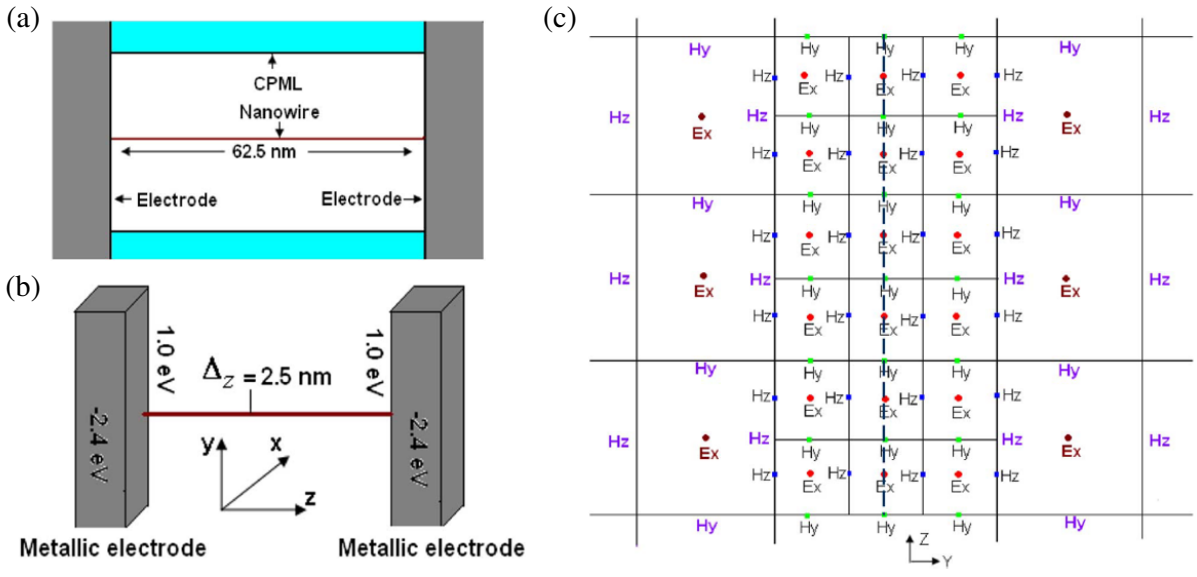

Figure 3. (a) Side view of the nanowire. (b) 3D structure of the nanowire connected to electrodes. (c) Fine mesh around nanowire, and coarse mesh in the rest of the region [28].

$$\frac{\partial D_x^{n+\frac{1}{3}}}{\partial t} + \sigma E_x^{n+\frac{1}{3}} = -J_x^{n+\frac{1}{3}}, \tag{26}$$

$$\frac{\partial D_y^{n+\frac{1}{3}}}{\partial t} + \sigma E_y^{n+\frac{1}{3}} = -\left(\frac{\partial H_z^{n+\frac{1}{3}}}{\partial x} - \frac{\partial H_z^{n}}{\partial x}\right) - J_y^{n+\frac{1}{3}}, \tag{27}$$

$$\frac{\partial D_z^{n+\frac{1}{3}}}{\partial t} + \sigma E_z^{n+\frac{1}{3}} = \left(\frac{\partial H_y^{n+\frac{1}{3}}}{\partial x} - \frac{\partial H_y^{n}}{\partial x}\right) - J_z^{n+\frac{1}{3}}. \tag{28}$$

The FDTD techniques used to solve TDSE have already been described in the previous section. The only difference is that in the presence of EM field, Eq. (3) needs to be modified as

$$i\hbar\frac{\partial\Psi(r,t)}{\partial t} = \left[\frac{1}{2m}[-i\hbar\nabla - qA(r,t)]^2 + q\Phi(r,t) + V(r,t)\right]\Psi(r,t). \tag{29}$$

where "**A**" and "Φ" represent vector and scalar potential terms, respectively, and satisfy

$$B = \nabla \times A, \tag{30}$$

$$E = -\nabla\Phi - \frac{\partial A}{\partial t}. \tag{31}$$

Due to the interface complexity, the TDSE is considered in 1D case, which can be written along the z-axis in terms of real and imaginary parts as [56]

$$\begin{aligned}\frac{\partial\Psi_R(z,t)}{\partial t} &= -\frac{\hbar}{2m}\frac{\partial^2\Psi_I(z,t)}{\partial^2 z} + \frac{q^2}{2\hbar m}A_z(z,t)^2\Psi_I(z,t) - \frac{q}{\hbar}\Phi(z,t)\Psi_I(z,t) + \frac{V(z)}{\hbar}\Psi_I(z,t)\\ &\quad -\frac{q}{m}A_z(z,t)\frac{\partial\Psi_R(z,t)}{\partial z} - \frac{q}{2m}\Psi_R(z,t)\frac{\partial A_z(z,t)}{\partial z},\end{aligned} \tag{32}$$

$$\begin{aligned}\frac{\partial\Psi_I(z,t)}{\partial t} &= \frac{\hbar}{2m}\frac{\partial^2\Psi_R(z,t)}{\partial^2 z} - \frac{q^2}{2\hbar m}A_z(z,t)^2\Psi_R(z,t) + \frac{q}{\hbar}\Phi(z,t)\Psi_R(z,t) - \frac{V(z,t)}{\hbar}\Psi_R(z,t)\\ &\quad -\frac{q}{m}A_z(z,t)\frac{\partial\Psi_I(z,t)}{\partial z} - \frac{q}{2m}\Psi_I(z,t)\frac{\partial A_z(z,t)}{\partial z}.\end{aligned} \tag{33}$$

After getting the solution of the TDSE, the quantum current density is given by

$$J_z(z,t) = -\frac{q}{2m}i\hbar\left(\Psi^*(z,t)\frac{\partial}{\partial z}\Psi(z,t) - \Psi(z,t)\frac{\partial}{\partial z}\Psi^*(z,t)\right) - \frac{q^2}{m}A_z|\Psi(z,t)|^2. \tag{34}$$

In this hybrid method, the time step in the LOD-FDTD region can be larger because implicit method is used. Thus, it has more freedom to choose time steps and is flexible in terms of synchronization in time steps compared with the traditional method like the explicit hybrid approach [31], in which the time step in the region where quantum effect exists and in the rest of the region needs to be the same to maintain stability [28].

Moreover, in the time-dependent EM-QM simulation, we are more concerned with how to select discrete unit size and what FDTD techniques are used in different regions to reach a good tradeoff between efficiency, accuracy and stability. And there are also many other numerical techniques to solve the Maxwell-TDSE coupled equations [56–61] such as the high-order symplectic FDTD scheme [32, 62], alternating direction implicit (ADI) FDTD method [63].

3. APPLICATIONS

In this section, the applications of FDTD method in the QS EM and time-dependent QM simulation for nanoscale semiconductor devices and in the time-dependent EM-QM simulation for optoelectronic devices are introduced [64–69].

3.1. FDTD for Nanoscale Semiconductor Devices

In 2006, Chen et al. applied the Poisson-TDSE coupled equations to study the time-dependent quantum transport and non quasi-static (NQS) effects in the coaxially gated carbon nanotube field-effect transistor (CNTFET) [1, 50]. The structure and corresponding simulation results are shown in Fig. 4 [50] and Fig. 5 [1, 50]. With the increase of frequency, the amplitudes of the small signal current and charge decrease, which mean the gate gradually loses control of the device. Besides, the validity of the QS approximation is also examined. The simulation results show that at high frequencies, the QS

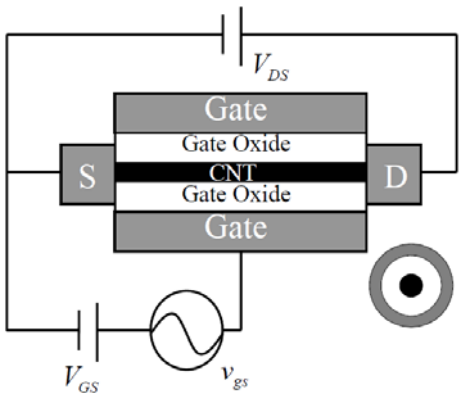

Figure 4. Structure of the coaxially gated carbon nanotube field effect transistor [50].

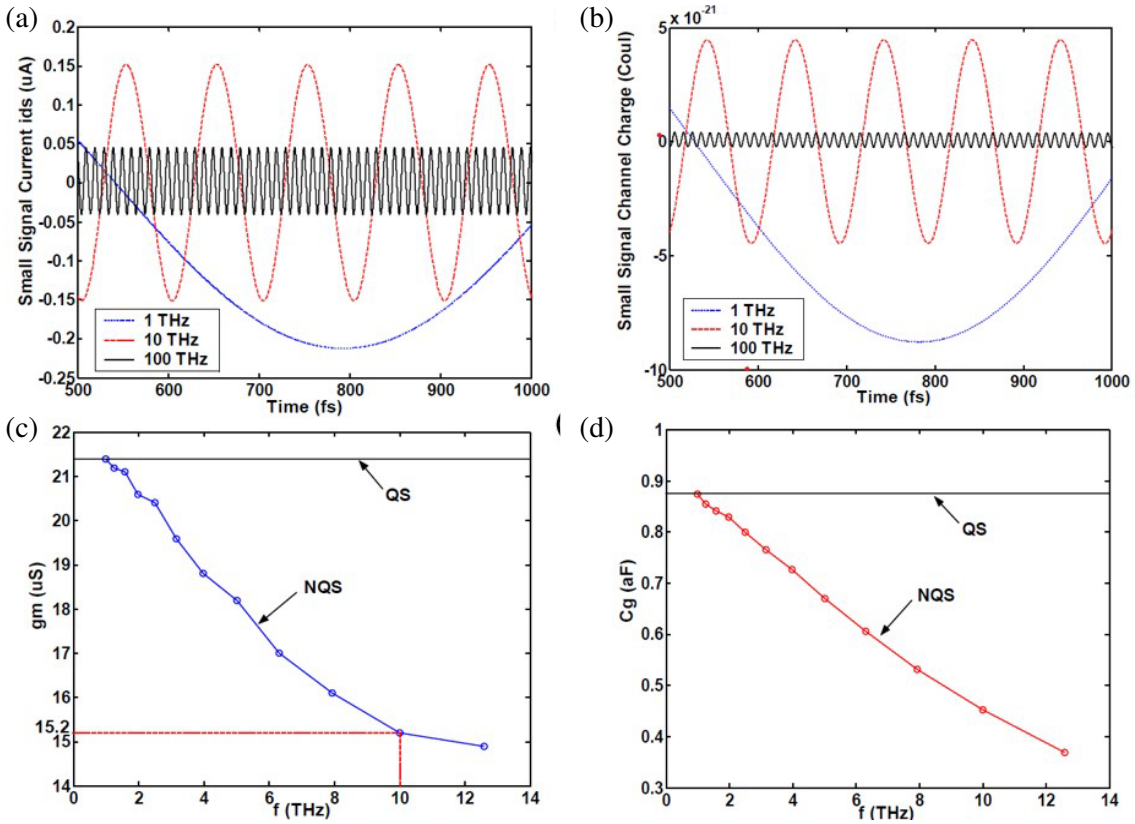

Figure 5. (a) Small signal time-dependent drain to source current and (b) small signal time-dependent channel charge at $V_{DS} = 0.5\,V$, $V_{GS} = 0.5\,V$, $v_{gs} = 10\,mV$. (c) AC transconductance and (d) gate capacitance versus frequency at $V_{DS} = 0.5\,V$, $V_{GS} = 0.5\,V$ [1, 50].

approach overestimates the transconductance and gate capacitance and is not accurate, thus, fails to explore the NQS effects in the CNTFET.

In 2008, Chen et al. also solved the Poisson-TDSE coupled equations to simulate the dynamic properties of CNTFET [26]. The time evolutions of the total charge density and current of the CNTFET in response to different gate voltages are shown in Fig. 6 [26]. From the simulation results, we can see the charge density and current respond to the variation of the applied voltages simultaneously. When a higher gate voltage is applied, the current overshoot is greater than its steady-state value and will take more time to stabilize.

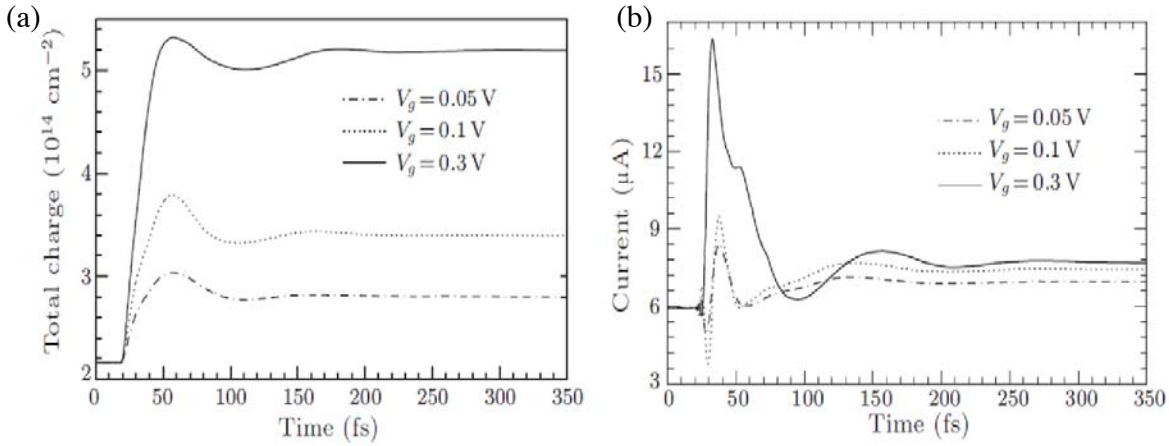

Figure 6. (a) Time evolution of total charge density in response to different gate voltages. (b) Time evolution of current in the center of the device in response to different gate voltages [26].

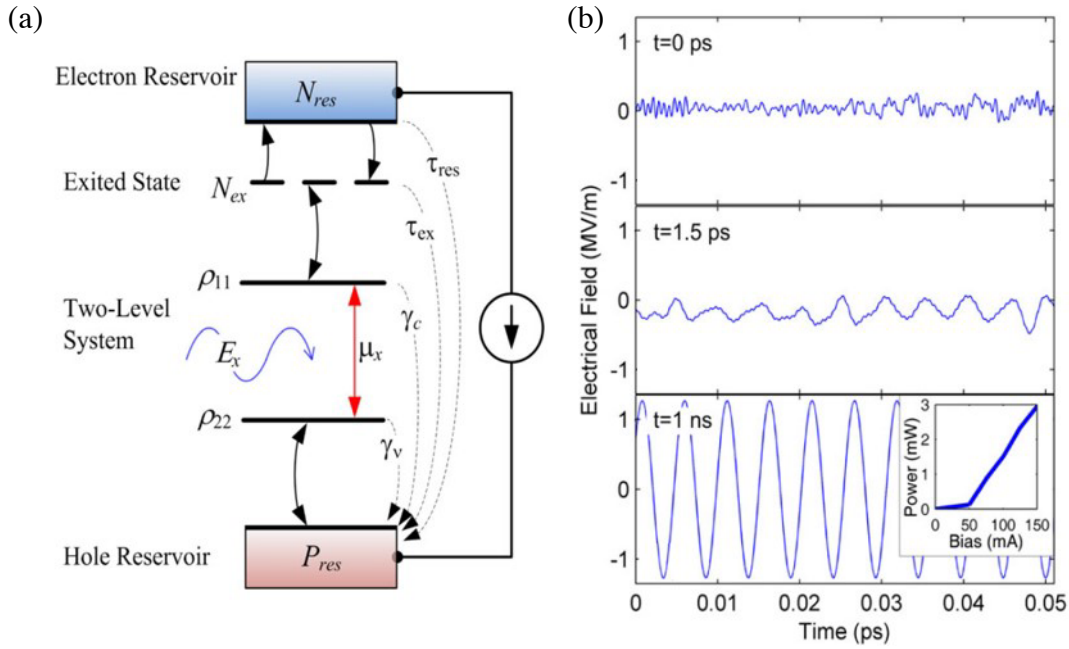

Figure 7. (a) Schematic diagram of the energetic structure of a QD in a carrier reservoir. (b) Emitted electric field at different time of the calculation, $t = 0$, $t = 1.5$ ps, $t = 1$ ns. The inset shows the emitted output power versus bias level [3].

3.2. FDTD for Optoelectronic Devices

FDTD method can be used for simulation of various optoelectronic devices, such as plasmonic devices [33], QD lasers and SOAs [3, 34, 35, 70–72], and devices for quantum states control [37, 38, 73]. In 2013, Capua et al. used FDTD method to simulate the dynamic properties of QD lasers and SOAs by solving the Maxwell-TDSE coupled equations [3]. In QD lasers and SOAs, the QD active gain medium is modeled by a two-level system interacting with the EM field, as shown in Fig. 7(a) [3]. The build-up of laser oscillations is presented in Fig. 7(b) [3]. It is seen that the steady-state oscillations are established after the energetic transition processes are completed. Besides, the well-known properties such as relaxation oscillations can be also seen from the simulation. Then, applying an antireflection coating, the QD laser can be turned into a SOA. The amplification of ultrashort pulses and the Rabi-oscillation phenomenon in SOA are also studied [3]. Rabi-oscillation is a very important regime in the device, that is when the particle (or two-level system) is illuminated by EM waves in a cavity, it cyclically absorbs photons and re-emits them by stimulated emission [74]. And the impacts of field intensity, detuning, and material loss on the population inversion in Rabi-oscillation regime were further investigated and discussed by Chen et al. in 2015 [34].

In addition, the control of quantum states [38, 74–76] has attracted great attention for various applications such as quantum computaion [77–79]. In 2015, Takeuchi et al. proposed a scheme of

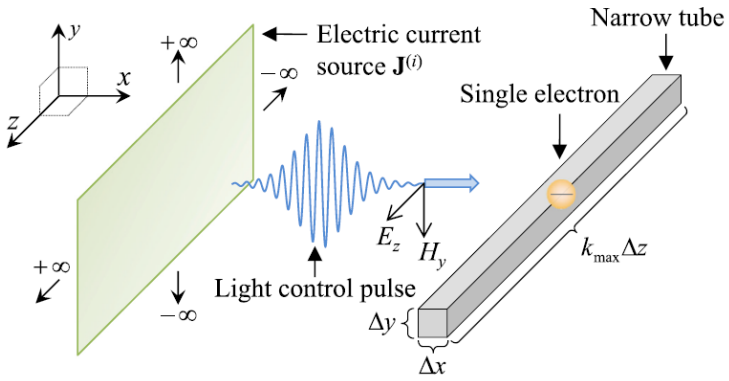

Figure 8. The model of a single electron confined in a quasi-1D nanoscale potential well and irradiated by a pulsed laser field. The electric current source of the incident laser pulse is distributed uniformly on the y-z plane and excites a plane-wave light control pulse polarized along z axis [37].

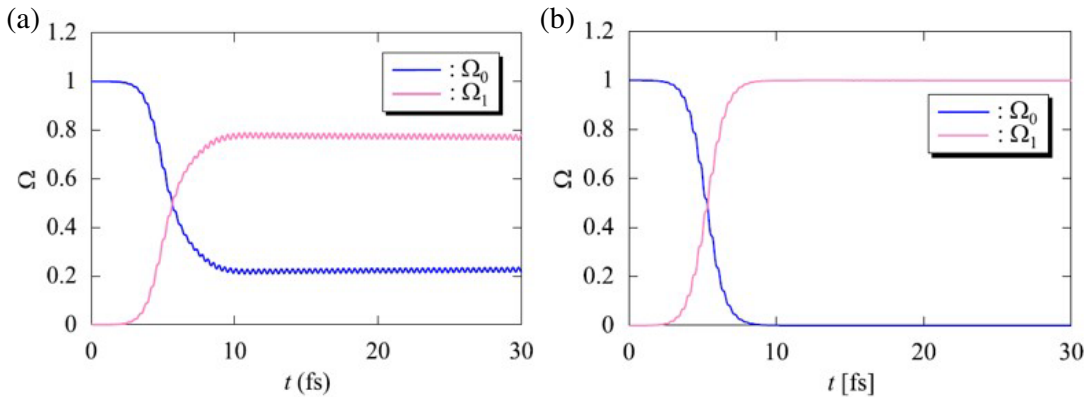

Figure 9. The temporal variation of the ground state Ω_0 and the objective state Ω_1 in the time-dependent electron wave packet obtained by the Maxwell-TDSE hybrid simulation employing (a) the conventional light control pulse and (b) the present light control pulse [37].

designing laser pulses for controlling quantum states based on the Maxwell-TDSE hybrid simulation [37]. A typical example is a single electron confined in a quasi-1D nanoscale potential well and irradiated by a pulsed laser field, as shown in Fig. 8 [37]. The simulated temporal variations of the ground state Ω_0 and the objective state Ω_1 are shown in Fig. 9 [37]. It indicates that the present light control pulse can effectively control the quantum states by considering the feedback from the excited electrons which could yield a locally strong EM field, also called near-field, in the vicinity of the target electron system [80–82]. Moreover, they applied the hybrid simulation to predict the influence of the near-field in the optical control of confined electron systems in 2017 [73], from which one can investigate and predict how strongly the near-field generated by the excited electrons affects the light control pulse. And it also shows that the near-field effects have strong dependence on the characteristics of the laser pulse and the confined electron systems, such as amplitude of the light control pulse, electron density, and length of the nanotube. In 2018, Yang et al. simulated the multi-quantum state control of nanotube by solving the Maxwell-TDSE coupled equations, and the probability distribution of electrons and the conversion rate of electronic state in the nanotube are shown in Fig. 10 [36].

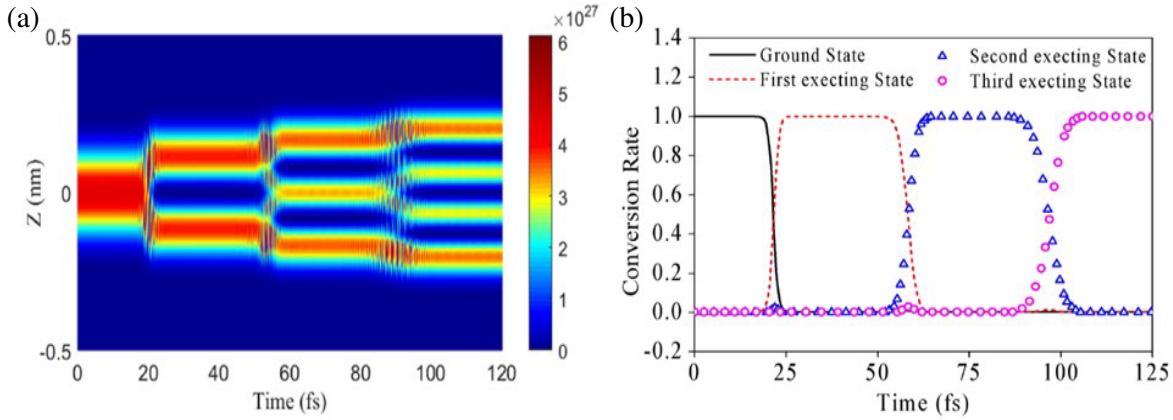

Figure 10. (a) Probability distribution of electrons in the nanotube. (b) Conversion rate of electronic states in the nanotube [36].

4. CONCLUSION

In summary, modeling and numerical simulation techniques for nanoscale semiconductor devices and optoelectronic devices to capture the interactions between EM and QM are necessary. FDTD method is effective to solve the Poisson-TDSE and the Maxwell-TDSE coupled equations in nanoscale semiconductor devices and optoelectronic devices. People have developed various discretization techniques to improve the performance of FDTD methods.

In terms of future research trends, there are many potential possibilities. First, the Maxwell-TDSE coupled model can be applied to a more complex system, maybe for electronic devices with a large quantity of electrons and holes, or in a more complex environment with inhomogeneous and nonlinear medium which will make an important impact on the transition dynamics. Second, nano-transistors or new nanodevices have received considerable research attention in recent years. The numerical simulation to study the high frequency transient performances of these devices is needed, and using the FDTD method to solve the TDSE with Poisson's equation is a good choice. Third, with the rapid development of the electronics industry, the system complexity has brought great challenges to the performance of the numerical algorithm. There is an urgent need for a more flexible FDTD technique with higher efficiency, accuracy, and stability for the device simulations. Finally, exploration of new mechanisms, and implementing it with the Maxwell-TDSE coupled equations to give a more complete description about the dynamic behaviors of the devices and systems are also very attractive.

ACKNOWLEDGMENT

The work is supported by the National Natural Science Foundation of China under Grants No. 61971375, 62071418 and 61931007, the Zhejiang Provincial Natural Science Foundation of China under Grant No. LR21F010003, and by the Opening Project of Science and Technology on Reliability Physics and Application Technology of Electronic Component Laboratory.

REFERENCES

1. Chen, Y., Y. Ouyang, J. Guo, and T. X. Wu, "Time-dependent quantum transport and nonquasistatic effects in carbon nanotube transistors," *Applied Physics Letters*, Vol. 89, 203122, 2006.
2. Chen, Y. P., W. E. I. Sha, W. C. H. Choy, L. Jiang, and W. C. Chew, "Study on spontaneous emission in complex multilayered plasmonic system via surface integral equation approach with layered medium Green's function," *Optics Express*, Vol. 20, No. 18, 20210, 2012.
3. Capua, A., O. Karni, and G. Eisenstein, "A finite-difference time-domain model for quantum-dot lasers and amplifiers in the Maxwell-Schrödinger framework," *IEEE Journal of Selected Topics in Quantum Electronics*, Vol. 19, No. 5, 1–10, 2013.
4. Yankwich, P. E., "Introduction to quantum mechanics," *Journal of the American Chemical Society*, Vol. 82, No. 14, 3803–3803, 1960.
5. Rae, A. I. M., "The picture book of quantum mechanics," *Physics Today*, Vol. 49, No. 1, 65–66, 1996.
6. Chan, T. F., D. Lee, and L. Shen, "Stable explicit schemes for equations of the Schrödinger type," *SIAM Journal on Numerical Analysis*, Vol. 23, No. 2, 274–281, 1986.
7. Chen, J. B. and M. Z. Qinz, "Multi-symplectic Fourier pseudospectral method for the nonlinear Schrödinger equation," *Electronic Transactions on Numerical Analysis Etna*, Vol. 12, 193–204, 2001.
8. Chang, Q. and G. Wang, "Multigrid and adaptive algorithm for solving the nonlinear Schrödinger equation," *Journal of Computational Physics*, Vol. 85, No. 2, 504, 1989.
9. Dai, W. Z. and R. Nassar, "A finite difference scheme for the generalized nonlinear Schrödinger equation with variable coefficients," *Journal of Computational Mathematics*, Vol. 18, No. 2, 123–132, 2000.
10. Delfour, M., M. Fortin, and G. Payr, "Finite-difference solutions of a non-linear Schrödinger equation," *Journal of Computational Physics*, Vol. 44, No. 2, 277–288, 1981.
11. Herbst, B. M., J. Ll Morris, and A. R. Mitchell, "Numerical experience with the nonlinear Schrödinger equation," *Journal of Computational Physics*, Vol. 60, No. 2, 282–305, 1985.
12. Taflove, A. and S. C. Hagness, *Computational Electrodynamics (The Finite-difference Time-domain Method)*, 3rd Edition, Artech House, 2001.
13. Sullivan, D. M., *Electromagnetic Simulation Using the FDTD Method*, 2nd Edition, Chapters 1–11, Wiley-IEEE Press, 2000.
14. Sullivan, D. and D. S. Citrin, "Time-domain simulation of two electrons in a quantum dot," *Journal of Applied Physics*, Vol. 89, No. 7, 3841–3846, 2001.
15. Sullivan, D. M. and D. S. Citrin, "Determination of the eigenfunctions of arbitrary nanostructures using time domain simulation," *Journal of Applied Physics*, Vol. 91, No. 5, 3219–3226, 2002.
16. Soriano, A., E. A. Navarro, J. A. Porti, and V. Such, "Analysis of the finite difference time domain technique to solve the Schrödinger equation for quantum devices," *Journal of Applied Physics*, Vol. 95, No. 12, 8011–8011, 2004.
17. Sudiarta, I. W. and D. J. W. Geldart, "Solving the Schrödinger equation using the finite difference time domain method," *Journal of Physics A: Mathematical and Theoretical*, Vol. 40, No. 8, 1885–1896, 2007, doi: 10.1088/1751-8113/40/8/013.

18. Moxley, F. I., D. T. Chuss, and W. Dai, "A generalized finite-difference time-domain scheme for solving nonlinear Schrödinger equations," *Computer Physics Communications*, Vol. 184, No. 8, 1834–1841, 2013.
19. Tay, W. C. and E. L. Tan, "Pentadiagonal alternating-direction-implicit finite-difference time-domain method for two-dimensional Schrödinger equation," *Computer Physics Communications*, Vol. 185, No. 7, 1886–1892, 2014.
20. Wilson, J. P. and W. Dai, "Generalized finite-difference time-domain method with absorbing boundary conditions for solving the nonlinear Schrödinger equation on a GPU," *Computer Physics Communications*, Vol. 235, 279–292, 2019.
21. Dai, W., G. Li, R. Nassar, and S. Su, "On the stability of the FDTD method for solving a time-dependent Schrödinger equation," *Numerical Methods for Partial Differential Equations*, Vol. 21, No. 6, 1140–1154, 2010.
22. Adamowski, J., "A numerical solution of the Poisson-Schrödinger problem for a vertical gated quantum dot," *TASK Quarterly*, Vol. 8, 603, 2004, doi: 10.13140/2.1.4912.7040.
23. Fiori, G. and G. Iannaccone, "The effect of quantum confinement and discrete dopants in nanoscale 50 nm n-MOSFETs: A three-dimensional simulation," *IEEE Transactions on Nanotechnology*, Vol. 13, No. 3, 294, 2002, doi: 10.1088/0957-4484/13/3/311.
24. Guo, J., et al., "Assessment of high-frequency performance potential of carbon nanotube transistors," *IEEE Transactions on Nanotechnology*, Vol. 4, No. 6, 715–721, 2005.
25. Stefanucci, G., S. Kurth, A. Rubio, and E. K. U. Gross, "Time-dependent approach to electron pumping in open quantum systems," *Physical Review B*, Vol. 77, 75339, 2008, doi: 10.1103/PhysRevB.77.075339.
26. Chen, Z.-D., J.-Y. Zhang, and Z.-P. Yu, "Time-dependent transport in nanoscale devices," *Chinese Physics Letters*, Vol. 26, No. 3, 37303–37306(4), 2009.
27. Yang, J. and W. Sui, "Solving Maxwell-Schrödinger equations for analyses of nano-scale devices," *European Microwave Conference*, 2007.
28. Ahmed, I., E. H. Khoo, E. Li, and R. Mittra, "A hybrid approach for solving coupled Maxwell and Schrödinger equations arising in the simulation of nano-devices," *IEEE Antennas and Wireless Propagation Letters*, Vol. 9, 914–917, 2010, doi: 10.1109/lawp.2010.2076411.
29. Shibayama, J., M. Muraki, J. Yamauchi, and H. Nakano, "Efficient implicit FDTD algorithm based on locally one-dimensional scheme," *Electronics Letters*, Vol. 41, No. 19, 1046–1047, 2006.
30. Ahmed, I., E. K. Chua, E. P. Li, and Z. Chen, "Development of the three-dimensional unconditionally stable LOD-FDTD method," *IEEE Transactions on Antennas and Propagation*, Vol. 58, No. 11, 832–837, 2010.
31. Pierantoni, L., D. Mencarelli, and T. Rozzi, "A new 3-D transmission line matrix scheme for the combined Schrödinger-Maxwell problem in the electronic/electromagnetic characterization of nanodevices," *IEEE Transactions on Microwave Theory and Techniques*, Vol. 56, No. 3, 654–662, 2008.
32. Xiang, C., F. Kong, K. Li, and M. Liu, "A high-order symplectic FDTD scheme for the Maxwell-Schrödinger system," *IEEE Journal of Quantum Electronics*, Vol. 54, No. 1, 1–8, 2018.
33. Lee, K. H., I. Ahmed, R. S. M. Goh, E. H. Khoo, E. P. Li, and T. G. G. Hung, "Implementation of the FDTD method based on Lorentz-Drude dispersive model on GPU for plasmonics applications," *Progress In Electromagnetics Research*, Vol. 116, 441–456, 2011.
34. Chen, Y. P., Y. M. Wu, and W. E. I. Sha, "Modeling Rabi oscillation by rigorously solving Maxwell-Schrödinger equation," *IEEE International Symposium on Microwave*, 2016.
35. Hatori, N., M. Sugawara, T. Akiyama, and Y. Nakata, "Low frequency chirp self-assembled InGaAs/GaAs quantum dot lasers," *Lasers & Electro-optics Society, Leos the Meeting of the IEEE*, 2001.
36. Yang, Z. D., L. Zhang, H. Zeng, D. Z. Ding, and R. S. Chen, "Multi-quantum state control of nano-tube by the Maxwell-Schrödinger hybrid method," *2018 Cross Strait Quad-Regional Radio Science and Wireless Technology Conference (CSQRWC)*, 2018.

37. Takeuchi, T., S. Ohnuki, and T. Sako, "Maxwell-Schrödinger hybrid simulation for optically controlling quantum states: A scheme for designing control pulses," *Physical Review A*, Vol. 91, No. 3, 033401, 2015.
38. Meshulach, D. and Y. Silberberg, "Coherent quantum control of two-photon transitions by a femtosecond laser pulse," *Nature*, Vol. 396, No. 6708, 239–242, 1998.
39. Chen, Z., J. Zhang, and Z. Yu, "Solution of the time-dependent Schrödinger equation with absorbing boundary conditions," *Journal of Semiconductors*, Vol. 30, No. 1, 1–6, 2009.
40. Subasi, M., "On the finite-differences schemes for the numerical solution of two dimensional Schrödinger equation," *Numerical Methods for Partial Differential Equations*, Vol. 18, No. 6, 752–758, 2002, doi: 10.1002/num.10029.
41. Burden, R. L. and J. D. Faires, *Numerical Analysis*, 5th Edition, PWS Publishing Co., 1988.
42. Visscher, P. B., "A fast explicit algorithm for the time-dependent Schrödinger equation," *Computers in Physics*, Vol. 5, No. 6, 596–598, 1991.
43. Tal-Ezer, H. and R. Kosloff, "An accurate and efficient scheme for propagating the time dependent Schrödinger equation," *Journal of Chemical Physics*, Vol. 81, No. 9, 3967–3971, 1984.
44. Leforestier, C., et al., "A comparison of different propagation schemes for the time dependent Schrödinger equation," *Journal of Computational Physics*, Vol. 94, No. 1, 59–80, 1991.
45. Leforestier, C., R. H. Bisseling, C. Cerjan, M. D. Feit, and R. Kosloff, "A comparison of different propagation schemes for the time dependent Schrödinger equation," *Journal of Computational Physics*, Vol. 89, No. 1, 490–491, 1991.
46. De Raedt, H., K. Michielsen, J. S. Kole, and M. T. Figge, "One-step finite-difference time-domain algorithm to solve the Maxwell equations," *Physical Review E Statal Nonlinear & Soft Matter Physics*, Vol. 67, No. 5, Pt. 2, 056706, 2003.
47. Bar-On, I. and M. Leoncini, "Stable solution of tridiagonal systems," *Numerical Algorithms*, Vol. 18, No. 3, 361–388, 1998, doi: 10.1023/A:1019137919461.
48. Zhang, Y., J. Cohen, A. A. Davidson, and J. D. Owens, "A hybrid method for solving tridiagonal systems on the GPU," *GPU Computing Gems Jade Edition*, 117–132, 2012.
49. Chen, Y. C. and C. R. Lee, *Augmented Block Cimmino Distributed Algorithm for Solving Tridiagonal Systems on GPU*, Chapter 9, Advances in GPU Research and Practice, 2017.
50. Chen, Y., "Finite element method modeling of advanced electronic devices," Electronic Theses and Dissertations, 2006.
51. Alsunaidi, M. A., S. M. S. Imtiaz, and S. M. El-Ghazaly, "Electromagnetic wave effects on microwave transistors using a full-wave time-domain model," *IEEE Transactions on Microwave Theory and Techniques*, Vol. 44, No. 6, 799–808, 1996.
52. Grondin, R. O., S. M. El-Ghazaly, and S. M. Goodnick, "A review of global modeling of charge transport in semiconductors and full-wave electromagnetics," *IEEE Transactions on Microwave Theory and Techniques*, Vol. 47, No. 11, 2167–2167, 2002.
53. Naeemi, A., R. Sarvari, and J. D. Meindl, "Performance comparison between carbon nanotube and copper interconnects for GSI," *IEEE International Electron Devices Meeting*, 2005.
54. Kim, G., E. Arvas, V. Demir, and A. Z. Elsherbeni, "A novel nonuniform subgridding scheme for FDTD using an optimal interpolation technique," *Progress In Electromagnetics Research B*, Vol. 44, 137–161, 2012.
55. Mailloux, R., "Theory of electromagnetic waves," *IEEE Antennas & Propagation Society Newsletter*, Vol. 26, No. 2, 13–14, 1984.
56. Ahmed, I. and E. Li, "A hybrid FDTD and ADI-FDTD technique for coupled Maxwell's and Schrödinger's equations," *IEEE Antennas & Propagation Society International Symposium*, 2010.
57. Ren, X., et al., "High-order unified symplectic FDTD scheme for the metamaterials," *Computer Physics Communications*, Vol. 183, No. 6, 1192–1200, 2012.
58. Ryu, C. J., A. Liu, W. E. I. Sha, and W. C. Chew, "Finite-difference time-domain simulation of the Maxwell-Schrödinger system," *IEEE Journal on Multiscale & Multiphysics Computational Techniques*, Vol. 1, 40–47, 2016.

59. Ryu, C. J., A. Y. Liu, W. E. I. Sha, and W. C. Chew, "Finite-difference time-domain simulation of the Maxwell-Schrödinger system," *IEEE Journal on Multiscale and Multiphysics Computational Techniques*, Vol. 1, 40–47, 2016, doi: 10.1109/JMMCT.2016.2605378.
60. Turati, P., "FDTD modelling of nanostructures at microwave frequency," *Surface & Coatings Technology*, Vol. 254, No. 10, 402–409, 2014.
61. Pierantoni, L., D. Mencarelli, and T. Rozzi, "The combined Schrödinger-Maxwell problem in the electronic/electromagnetic characterization of nanodevices," *Time Domain Methods in Electrodynamics*, 105–133, 2008.
62. Xie, G., Z. Huang, M. Fang, and W. Sha, "Simulating Maxwell-Schrödinger equations by high-order symplectic FDTD algorithm," *IEEE Journal on Multiscale and Multiphysics Computational Techniques*, Vol. 4, 143–151, 2019, doi: 10.1109/JMMCT.2019.2920101.
63. Zheng, F. and Z. Chen, "A finite-difference time-domain method without the Courant stability conditions," *IEEE Microw. Guided Wave Lett.*, Vol. 9, No. 11, 441–443, 1999.
64. Ravi, K., Y. Huang, and S. Ho, "A computationally efficient, non-equilibrium, carrier temperature dependent semiconductor gain model for FDTD simulation of optoelectronic devices," *2011 Numerical Simulation of Optoelectronic Devices*, 113–114, Sep. 5–8, 2011, doi: 10.1109/NUSOD.2011.6041166.
65. Bhardwaj, S., "Electronic-electromagnetic multiphysics modeling for terahertz plasmonics: A review," *IEEE Journal on Multiscale and Multiphysics Computational Techniques*, Vol. 4, 307–316, 2019, doi: 10.1109/JMMCT.2019.2957361.
66. Wang, G., et al., "The numerical modeling of 3D microfiber couplers and resonators," *IEEE Photonics Technology Letters*, Vol. 28, No. 15, 1707–1710, 2016, doi: 10.1109/LPT.2016.2551323.
67. Tan, E. L. and D. Y. Heh, "Multiple 1-D fundamental ADI-FDTD method for coupled transmission lines on mobile devices," *IEEE Journal on Multiscale and Multiphysics Computational Techniques*, Vol. 4, 198–206, 2019, doi: 10.1109/JMMCT.2019.2945187.
68. Zhai, M., H. Peng, J. Mao, and W. Yin, "Modeling tunable graphene-based filters using leapfrog ADI-FDTD method," *2015 IEEE MTT-S International Microwave Workshop Series on Advanced Materials and Processes for RF and THz Applications (IMWS-AMP)*, 1–3, Jul. 1–3, 2015, doi: 10.1109/IMWS-AMP.2015.7325025.
69. Bahl, M., et al., "Mixed-level simulation of opto-electronic devices," *2016 International Conference on Numerical Simulation of Optoelectronic Devices (NUSOD)*, 101–102, Jul. 11–15, 2016, doi: 10.1109/NUSOD.2016.7547050.
70. Bandrauk, E. L. C., "A numerical Maxwell-Schrödinger model for intense laser-matter interaction and propagation," *Computer Physics Communications*, 2007.
71. Navarro, D., "A carrier-transit-delay-based nonquasi-static MOSFET model for circuit simulation and its application to harmonic distortion analysis," *IEEE Transactions on Electron Devices*, Vol. 53, No. 9, 2025–2034, 2006.
72. Chen, Y. P., W. E. I. Sha, L. Jiang, M. Meng, Y. M. Wu, and W. C. Chew, "A unified Hamiltonian solution to Maxwell-Schrödinger equations for modeling electromagnetic field-particle interaction," *Computer Physics Communications*, Vol. 215, 63–70, 2017, doi: 10.1016/j.cpc.2017.02.006.
73. Takeuchi, T., S. Ohnuki, and T. Sako, "A simple formula to predict the influence of the near-field in the optical control of confined electron systems," *Journal of Physics B Atomic Molecular & Optical Physics*, Vol. 50, No. 4, 045002, 2017.
74. Gerry, C., *Introductory Quantum Optics*, 1st Edition, Cambridge University Press, London, 2004.
75. Rabitz, H., "Whither the future of controlling quantum phenomena?," *Science*, Vol. 288, No. 5467, 824–828, 2000.
76. Townsend, D., et al., "A Stark future for quantum control," *The Journal of Physical Chemistry A*, Vol. 4, No. 115, 357–373, 2011.
77. Rangan, C. and P. H. Bucksbaum, "Optimally shaped terahertz pulses for phase retrieval in a Rydberg-atom data register," *Physical Review A*, Vol. 64, No. 3, 033417, 2001, doi: 10.1103/PhysRevA.64.033417.

78. Palao, J. P. and R. Kosloff, "Quantum computing by an optimal control algorithm for unitary transformations," *Physical Review Letters*, Vol. 89, No. 18, 188301, 2002, doi: 10.1103/PhysRevLett.89.188301.
79. Nunn, J., et al., "Mapping broadband single-photon wave packets into an atomic memory," *Physical Review A*, Vol. 75, No. 1, 011401, 2007, doi: 10.1103/PhysRevA.75.011401.
80. Lewis, A. and K. Lieberman, "Near-field optical imaging with a non-evanescently excited high-brightness light source of sub-wavelength dimensions," *Nature*, Vol. 354, No. 6350, 214–216, 1991, doi: 10.1038/354214a0.
81. Zenhausern, F., "Apertureless near-field optical microscope," *Applied Physics Letters*, Vol. 65, No. 13, 1623–1625, 1994.
82. Choi, S., et al., "Active tailoring of nanoantenna plasmonic fields using few-cycle laser pulses," *Physical Review A*, Vol. 93, No. 2, 021405, 2016.